JOURNAL OF Materials CHEMISTRY

High photostability and quantum yield of nanoporous TiO_2 thin film electrodes co-sensitized with capped sulfides

Shu-ming Yang,[a] Chun-hui Huang,*[a] Jin Zhai,[b] Zhong-sheng Wang[a] and Lei Jiang[b]

[a]*State Key Laboratory of Rare Earth materials Chemistry and Applicatons, Peking University–The University of Hong Kong Joint Laboratory in Rare Earth Materials and Bio-inorganic Chemistry, Peking University, Beijing 100871, PR China. E-mail: hch@chem.pku.edu.cn; Fax: +86-(10)62751708; Tel: +86-(10)62757156*

[b]*The Organic Solid Laboratory, Research Center of Molecular Science, Institute of Chemistry, The Chinese Academy of Science, Beijing 100871, PR China*

Received 3rd July 2001, Accepted 14th December 2001
First published as an Advance Article on the web 11th March 2002

Photoelectrochemical electrodes have been prepared by sequential deposition of quantum sized PbS, CdS and ZnS particles on TiO_2 nanocrystalline films. Their photoelectrochemical properties have been studied in a two-electrode system which conforms more closely to practical conditions. The results show that the ternary sulfide PbS/CdS/ZnS co-sensitized TiO_2 electrode generates incident photon-to-current conversion efficiency (IPCE) as high as nearly 100% under irradiation with 400 nm light; moreover its photostability is strongly improved, and this is the first report of this so far. The highest photoelectrical conversion efficiency is obtained for the TiO_2/PbS/CdS/ZnS electrode, and is about twice as much as that of TiO_2/PbS.

1 Introduction

Inorganic[1–10] and organic[11–27] materials have been extensively investigated in the sensitization of nanocrystalline semiconductor thin films for developing highly efficient photoelectrochemical cells[28,29] since Grätzel and his coworkers reported a solar cell based on a ruthenium complex adsorbed on highly porous nanocrystalline TiO_2 film.[1]

Sulfides of some metal ions, such as PbS, CdS, Bi_2S_3, Ag_2S *etc.*, can be promising candidates as sensitizers for wide bandgap semiconductors. The sulfide particles, fabricated on the surface of nanoporous TiO_2 by chemical deposition, are generally nanometres large. They demonstrate an obvious size quantization effect and their bandgaps are adjustable by a change in their particle sizes.[30] As a result, they are usually called quantum sized particles, abbreviated as Q-sulfides. On the other hand these sulfides are generally narrow bandgap semiconductors and absorb light efficiently. Compared with other sulfides, the advantage of PbS as a sensitizer lies in its high efficiency of light to electricity conversion. An incident photon-to-current conversion efficiency (IPCE) as high as 70% was reported for a TiO_2 electrode coated with Q-PbS, but the electrode experienced quick decay of photocurrent under irradiation.[30] It was found that the particle size of colloidal Q-PbS was increased upon illumination.[31] The formation of electrons and holes upon illumination seems to be accompanied by photochemical corrosion:

$$(PbS)_n \rightarrow (PbS)_{n-1} + Pb^{2+} + S^{2-}$$

The released Pb^{2+} and S^{2-} ions subsequently deposit on larger particles. Consequently the edge of the conduction band of Q-PbS went down even below that of TiO_2 and the charge carriers could not be transferred from Q-PbS to TiO_2 efficiently. We have found that the sizes of Q-PbS particles on TiO_2 film also increase under illumination and the photostability of Q-PbS particles can be enhanced to some extent after modification with thiols.[32] So the enhancement of photostability is an attractive subject in this area.

In this paper, nanocrystalline TiO_2 electrodes were fabricated and then subsequently modified with quantum sized PbS, CdS and ZnS particles by chemical deposition, and characterized with absorption spectra and AFM. Their photoelectrochemical properties were studied in a two-electrode system which conforms more closely to practical conditions than a three-electrode system. High photostability and high quantum yield of coupled electrodes were obtained.

2 Experimental

2.1 Materials and solutions

Water ($R \approx 18$ MΩ) from an Easy Pure RF System is used in the preparation of all solutions. All chemicals are reagent grade and used as received. 0.5 M Na_2S–0.1 M Na_2SO_3 aqueous solution is the supporting electrolyte in photoelectrochemical measurements.

2.2 Preparation of nanoporous TiO_2 thin film electrode

TiO_2 colloidal solution was prepared using a similar procedure to that described in ref. 1. In this work, the suspension of colloidal TiO_2 with a concentration of 120 g dm^{-3} is dispersed ultrasonically before use. Four drops, *ca.* 0.2 cm^3, of the suspension are applied onto a piece of transparent conducting glass (10 cm × 2.0 cm, fluorine-doped SnO_2, 30 Ω sq^{-1}) and spread uniformly. The sample was dried in air, then sintered at 450 °C for 30 min, and finally cooled to room temperature. The TiO_2 thin film is dipped in 0.2 mol dm^{-3} $TiCl_4$ aqueous solution for over 24 h and again sintered at 450 °C for 30 min. The thickness of electrode films was about 5 μm, measured with Tencor Alpha-Step Profiler.

2.3 Fabrication of electrodes co-sensitized with capped sulfides

The titanium dioxide thin film electrode was dipped into a saturated $Pb(NO_3)_2$ solution for 1 min, washed with water thoroughly, followed by dipping into 0.1 M Na_2S solution for 2 min and washing with water at least 3 times. This coating procedure with PbS was repeated up to several times as needed. Quantum sized CdS and ZnS are subsequently deposited onto

the Q-PbS modified TiO_2 electrode with the same procedure using saturated $Cd(NO_3)_2$ or $Cd(NO_3)_2$ and $Zn(NO_3)_2$ solution instead of $Pb(NO_3)_2$ to form electrodes TiO_2/PbS/CdS or TiO_2/PbS/CdS/ZnS, respectively.

2.4 Apparatus

Absorption spectra are recorded on a UV-3100 spectrophotometer (Shimadzu, Japan). AFM images are taken with a commercial AFM setup (Seiko SPA 3700N) under ambient conditions. All the images shown here are obtained in constant height mode, while precise height information is obtained from simultaneous constant force mode images. A triangular-shaped Si3N4 cantilever with a spring constant of 0.02 N m^{-1} is used to acquire images in contact mode. The applied force is typically 0.1 nN. Photoelectrochemical measurements are completed in a two electrode system. The modified TiO_2 thin films are used as working electrodes and a conductive glass with a layer of 200 nm thick platinum is used as the counter electrode. The source of excitation is a 500 W Xenon lamp. In order to get a given bandpass of light, the light beam is passed through a group of filters (Schott Co. USA). A KG4 filter (Schott) is set in the light beam to protect the electrodes from heating, and both WG360 and GG420 cut-off filters (Schott) to prevent the TiO_2 film from being excited by light with wavelength less than 420 nm. The light intensity is calibrated with a Light Gauge Radiometer/Photometer (Coherent, USA). The effective area for illumination is 0.2 cm^2.

3 Results and discussion

3.1 Construction of thin film modified electrodes

Fig. 1 shows the absorption spectra of a TiO_2 electrode after different numbers of coatings with Q-PbS and CdS. The general increase of absorption is clearly seen as well as the shifts of the absorption edges towards longer wavelengths with Q-PbS coating from one to three times. The shift to longer wavelength is explained by the size quantization effect. It was shown that the particle formation on the surface of the nanocrystalline TiO_2 film depends upon the interplay of the lattice energy of the particles and the adsorption of the metal ions at the surface, and the small particles formed during the first coating act as nucleation centers for the materials that are introduced in the next coating process.[9,33] The particle sizes of Q-PbS are estimated to be about 2.9, 4.0 and 4.8 nm for one, two and three coatings, respectively.[32] The curves labeled 4, 5, 6, 7 and 8 in Fig. 1 are ascribed to the absorption of CdS deposited on the PbS particles.

Once the TiO_2 thin film is modified with Q-PbS three times, another five coatings of CdS are deposited onto PbS. Our

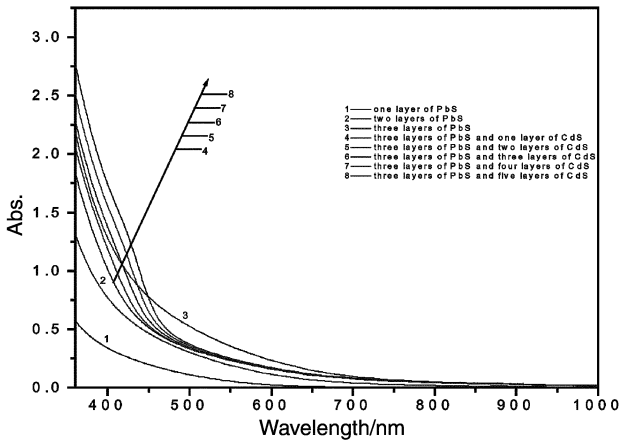

Fig. 1 Absorption spectra of a TiO_2 electrode after various numbers of coatings with Q-PbS and CdS.

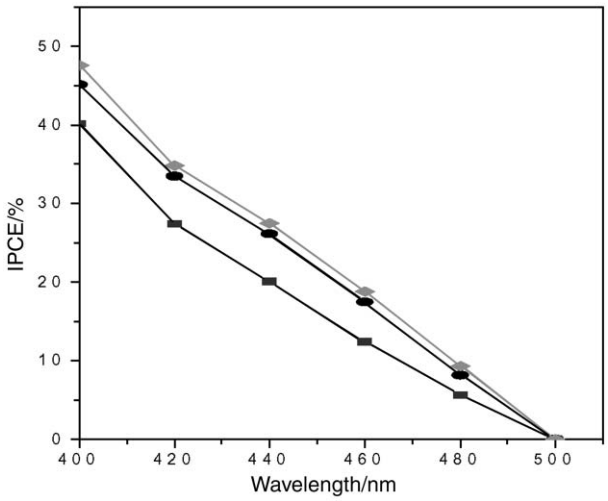

Fig. 2 Photocurrent action spectra of (■) TiO_2/three-layer CdS; (●) TiO_2/five-layer CdS; (◆) TiO_2/eight-layer CdS electrodes. The electrolyte is 0.5 M Na_2S and 0.1 M Na_2SO_3 aqueous solution, pH = 12.

previous work indicated that electrodes with three layers of PbS are able to generate the highest quantum yield,[32] so three layers of PbS are chosen in the present electrode fabrication, denoted as electrode TiO_2/PbS. On the other hand five layers of CdS are adopted to form capped electrodes because these electrodes are relatively efficient in both light absorption and photon-to-current conversion. Fig. 2 gives a comparison of the IPCE under different wavelengths for 3, 5 and 8 layers of CdS on TiO_2/PbS electrodes. The data show that the IPCE of the electrode with five-layer CdS is much better than that of the electrode with three-layer CdS and the IPCE changes little on modification from the five-layer up to eight-layer CdS. In order to keep the thickness suitable for electron transfer, the five layer CdS coating is selected in this work, denoted as electrode TiO_2/PbS/CdS. Finally three layers of ZnS are coated to form an outer layer to protect the PbS and CdS particles from photocorrosion, denoted as electrode TiO_2/PbS/CdS/ZnS. For comparison the electrode TiO_2/CdS is also prepared, which is constructed by coating five layers of CdS on TiO_2 film directly.

Fig. 3 shows the AFM images of the electrodes of the TiO_2 and TiO_2/PbS/CdS/ZnS thin films. It is clearly seen that the surface of the TiO_2 electrode is rather rough while that of the electrode TiO_2/PbS/CdS/ZnS appears relatively smooth. The mean grain sizes are measured with a computer to be 31.7 and 31.9 nm, and the mean roughness (RMS) 0.708 and 0.57 for the electrodes TiO_2 and TiO_2/PbS/CdS/ZnS respectively. These results can be understood by the fact that as the surface of nanoporous TiO_2 film is capped with sulfides the nanoporous holes are partly filled with the sulfide formed *in situ*, resulting in a decrease of the RMS.

3.2 Incident photo-to-current conversion efficiency

Short-circuit photocurrents are measured at various excitation wavelengths for several electrodes, and the IPCE is determined from the following expression

$$\mathrm{IPCE}(\%) = \frac{1240 \times J_{sc}/(\mu\mathrm{A} \times \mathrm{cm}^{-2})}{\lambda/\mathrm{nm} \times I_{inc}/(\mathrm{W} \times \mathrm{m}^{-2})} \quad (1)$$

where I_{inc} is the light flux incident on the electrode, J_{sc} is the short-circuit current and λ is the excitation wavelength.μ

The action spectra (Fig. 4) represent the IPCE *vs.* the various incident lights of different wavelength. In the case of TiO_2/CdS electrode, the highest IPCE is about 45% under irradiation with 400 nm light with 0.4 mW cm^{-2}, but it decreases to zero below 500 nm. On the other hand the highest IPCE of TiO_2/PbS electrode is about 45% under irradiation with 400 nm light, the

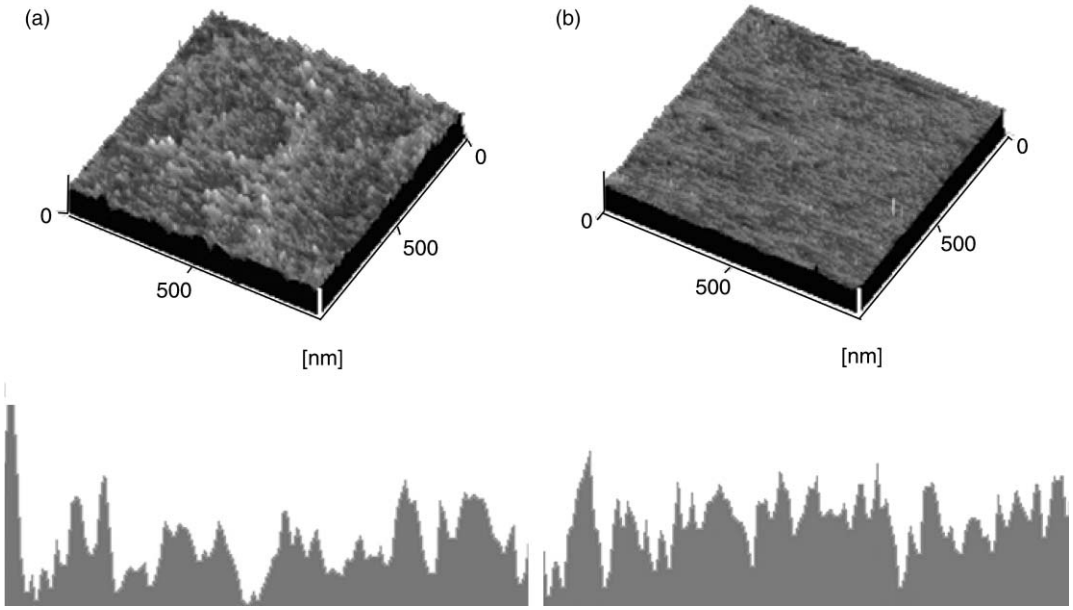

Fig. 3 The AFM images of electrodes: (a) TiO_2 and (b) TiO_2/PbS/CdS/ZnS showing surface morphology with the corresponding vertical height–distance profile bellow.

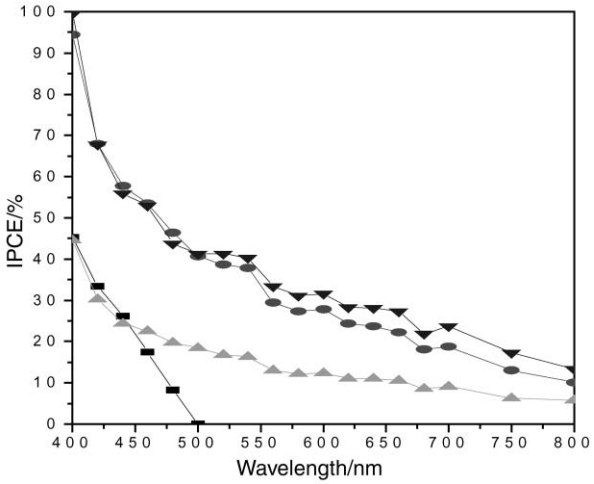

Fig. 4 Photocurrent action spectra of (▲) TiO_2/PbS; (■) TiO_2/CdS; (●) TiO_2/PbS/CdS; (▼) TiO_2/PbS/CdS/ZnS electrodes. The electrolyte is 0.5 M Na_2S and 0.1 M Na_2SO_3 aqueous solution, pH = 12.

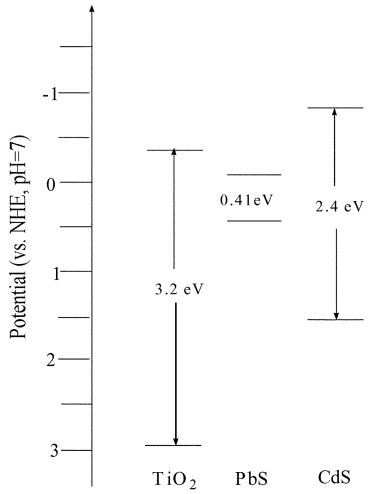

Scheme 1 Conduction band and valence band positions (*vs.* NHE, pH = 7) of TiO_2, CdS, PbS.

same as that of TiO_2/CdS electrode, however the IPCE is still about 10% even under irradiation with 800 nm light. When the TiO_2/PbS electrode is modified with CdS and ZnS, the IPCE of electrode TiO_2/PbS/CdS/ZnS at 400 nm nearly reaches 100 percent, which demonstrates that charge carriers are separated most efficiently with it.

The band positions of bulk PbS, CdS and TiO_2 are summarized in Scheme 1. The edge of the conduction band of bulk PbS lies below that of TiO_2, but as the size of PbS particles changes into the nanometre range, its conduction band would stand above that of TiO_2.[9] The edge of the conduction band of CdS is higher than that of TiO_2 and PbS. So the energetic differences between the conduction bands of the semiconductors bring about a driving force which facilitates the charge carrier transfer from the conduction bands of CdS and PbS then to that of TiO_2. The IPCE measurements, presented in Fig. 4, clearly demonstrate an increase in the photoresponse of two co-sensitized electrodes TiO_2/PbS/CdS and TiO_2/PbS/CdS/ZnS, proving a better charge separation, as a result of quick cascading of electrons from CdS to PbS, then to TiO_2.

3.3 Effect of light intensity

The photoelectrochemical behaviors of the electrodes are further evaluated by measuring short-circuit photocurrent and open-circuit photovoltage at various incident light intensities. The experimental results are presented in Fig. 5 and 6, respectively. It can be seen from the plot of J_{sc} *vs.* I_{inc} that the values of J_{sc} increase rapidly at lower incident intensities, then level off at higher incident intensities.

In Fig. 6 V_{oc} varies logarithmically with J_{sc}. This behavior reminds us of the photoelectrochemical cells employing crystal or polycrystalline electrodes operating on the Schottky barrier principle, where the space charge layer is present at the semiconductor/electrolyte interface and is responsible for charge separation. The relationship between V_{oc} and J_{sc} in such cells can be expressed by the following equation[34]

$$V_{oc} = (nkT/q)\ln [(J_{sc}/I_0) + 1] \quad (2)$$

where k, T, q and n are the Boltzmann constant, the thermodynamic temperature, the electronic charge, and the

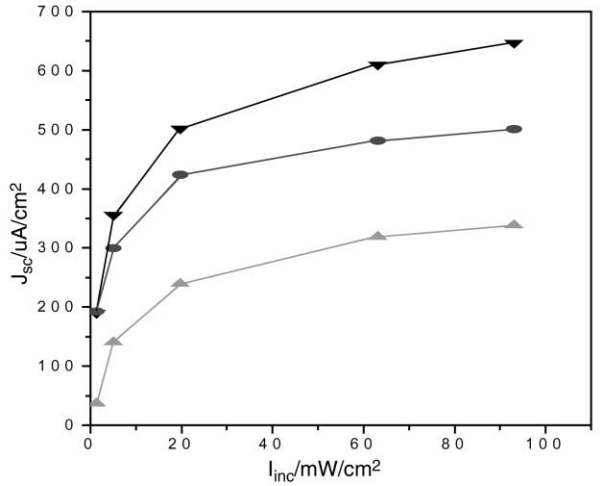

Fig. 5 Variation of short-circuit photocurrent J_{sc} as a function of incident light intensity I_{inc}. (▲) TiO_2/PbS; (●) TiO_2/PbS/CdS; (▼) TiO_2/PbS/CdS/ZnS electrodes. The electrolyte is 0.5 M Na_2S and 0.1 M Na_2SO_3 aqueous solution, pH = 12.

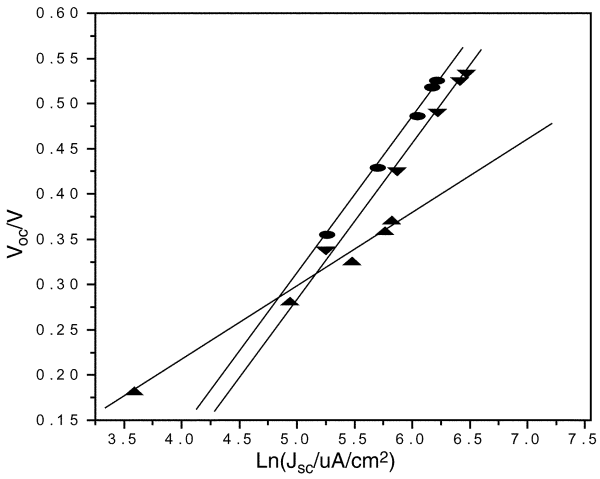

Fig. 6 Dependence of open-circuit photovoltage V_{oc} on incident light intensity. (▲) TiO_2/PbS; (●) TiO_2/PbS/CdS; (▼) TiO_2/PbS/CdS/ZnS. The electrolyte is 0.5 M Na_2S and 0.1 M Na_2SO_3 aqueous solution, pH = 12.

diode quality factor, respectively. I_0 is the reverse saturation current which results from the charge recombination and is a major disadvantage factor for V_{oc}. The dependence of V_{oc} on ln J_{sc} shows that eqn. (2) can be used to characterize the photoelectrochemical parameters of the electrodes. The values of n calculated from Fig. 4 are 3.17, 6.84 and 6.26, and the I_0 values 4.35, 28.5 and 25.9 μA cm^{-2} for the electrodes TiO_2/PbS, TiO_2/PbS/CdS, and TiO_2/PbS/CdS/ZnS respectively. The high values of reverse saturation current further highlight the problem of rectifying the flow of charge carriers in such sulfide-sensitized thin semiconductor films.

3.4 Photostability and photoelectrical conversion efficiency

Fig. 7 presents the photocurrent for three differently prepared electrodes *versus* illumination time (λ = 460 nm, 0.89 mW cm^{-2}).

It is seen that the photocurrent of the TiO_2/PbS electrode monotonically decreases from about 72.3 μA cm^{-2} in the beginning to 56.4 μA cm^{-2} after 4 hours' illumination, while the photostability is clearly improved for the TiO_2/PbS/CdS and TiO_2/PbS/CdS/ZnS electrodes. Their photocurrents stay unchanged at 171 and 182.4 μA cm^{-2} during 4 hours' illumination, respectively. It is known that the Q-CdS particles on TiO_2 show relatively high photostability and the photocurrent drops to half of the original value under illumination within weeks or months depending on preparation.[34] In our TiO_2/PbS electrode this occurs after a few hours. Once the TiO_2/PbS electrode is coated with CdS and ZnS which prevent the particle growth of Q-PbS, so its photostability is apparently enhanced and also its photocurrent greatly increases.

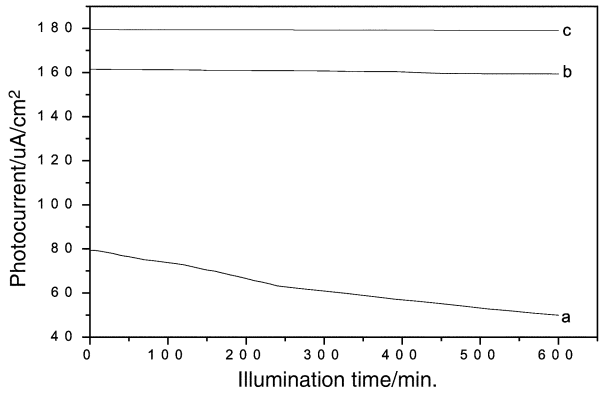

Fig. 7 Photocurrent for differently treated TiO_2 electrodes as a function of the illumination time with λ = 460 nm and I_{inc} = 0.89 mW cm^{-2}. (a) TiO_2/PbS; (b) TiO_2/PbS/CdS; (c) TiO_2/PbS/CdS/ZnS electrodes. The electrolyte is 0.5 M Na_2S and 0.1 M Na_2SO_3 aqueous solution, pH = 12.

Fig. 8 shows the photocurrent *versus* photovoltage diagrams of the three electrodes under illumination with 660 nm (Table 1). The short circuit photocurrent and open circuit photovoltage are increased after the modification of TiO_2/PbS electrodes with CdS or CdS and ZnS. For dye sensitized TiO_2

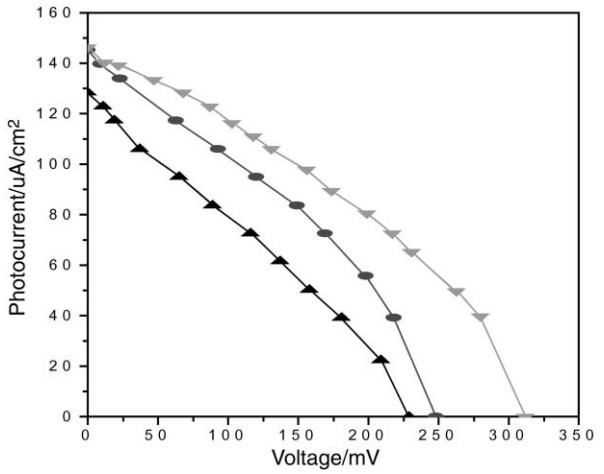

Fig. 8 The photocurrent–photovoltage diagrams of three electrodes under illumination with λ = 660 nm, I_{inc} = 1 mW cm^{-2}. (▲) TiO_2/PbS; (●) TiO_2/PbS/CdS; (▼) TiO_2/PbS/CdS/ZnS electrodes. The electrolyte is 0.5 M Na_2S and 0.1 M Na_2SO_3 aqueous solution, pH = 12.

Table 1 Photoelectrochemical parameters of sulfide-sensitized TiO_2 nanoporous solar cells[a]

Electrode	J_{sc}/ μA cm^{-2}	V_{oc}/ V	P_{max}/ μW cm^{-2}	ff[b]	η(%)
TiO_2/PbS	128.5	0.23	29.6	0.29	0.8
TiO_2/PbS/CdS	145.3	0.25	36.3	0.34	1.3
TiO_2/PbS/CdS/ZnS	146.4	0.31	45.4	0.35	1.6

[a]Measurements were carried out under irradiation with 660 nm incident with an illumination power of 1 mW cm^{-2}. [b]Fill factor.

cells the open circuit photovoltage is dynamically determined by the charge recombination at electrodes and electrolyte interface.[35,36] In our cases the values of V_{oc} increase in the order of TiO_2/PbS, TiO_2/PbS/CdS and TiO_2/PbS/CdS/ZnS electrodes, indicating that the charge recombination is largely suppressed in the case of the latter two electrodes.

4 Conclusion

In nanoporous semiconductor films, a rather unusual feature is the lack of a space charge layer.[37,38] As a result the charge recombination between electrons injected in the conduction band of the semiconductor and the oxidized sensitizer is one of the major limiting factors to the photoelectrical conversion efficiency. So the suppression of the charge recombination is a very important and challenging topic in this field. Our primary objective to envelop TiO_2 with PbS, CdS and ZnS is to exploit the beneficial role of the coupled arrangement in improving the process of charge separation in nanoporous semiconductor thin film electrodes as well as their photostability. The rationale behind this is that, in view of the conduction band of TiO_2 being at lower energy than that of PbS and the conduction band of PbS being at lower energy than that of CdS, the photogenerated electrons in CdS and PbS will be quickly transferred to TiO_2 while the holes remain in the valence bands, thus helping photogenerated electrons to escape recombination with holes and thereby improving the charge separation efficiency. The IPCE measurements in Fig. 4 clearly demonstrate an increase in the photoresponse of two co-sensitized electrodes TiO_2/PbS/CdS and TiO_2/PbS/CdS/ZnS, showing a better charge separation, as a result of quick cascading of electrons from CdS to PbS then to TiO_2. The higher photovoltages in co-sensitized electrodes are also the result of the improved charge separation in these systems.

As mentioned in the introduction, the other important objective of this work is to improve the photostability of quantum sized PbS on TiO_2 films. Photocorrosion is a major obstacle to its potential use in practical solar cells, and is mainly caused by the change of the particle sizes of PbS. For colloidal CdS particles it is known that coating the particles with thin layers of wide bandgap materials could lead to dramatic enhancement of the photostability.[39] The ZnS should be a proper candidate in modifying PbS and CdS. On one hand ZnS is a wide bandgap semiconductor (E_g = 3.6 eV) and stable under irradiation. On the other hand ZnS is similar in property to other sulfides and they can co-exist stably. So the ZnS layer is adopted to prevent the PbS and CdS from photocorrosion and to improve photostability. It is obviously seen from the photoelectrical results that the IPCE of the ZnS capped electrode TiO_2/PbS/CdS/ZnS reaches as high as nearly 100 percent under irradiation with light of 400 nm, and its energy conversion efficiency at a light of 660 nm is 1.8%, two times as much as that of the TiO_2/PbS electrode. Furthermore, its photocurrent stays almost unchanged during illumination.

From our results, the photocorrosion and the electron transport processes of the sulfide-sensitised cells are two of the important factors in the investigation of such materials for potential application. With the surface modification, the photostability and higher photoelectrical conversion efficiency of these electrodes are achieved. A major goal in further work will be the modification of surface states in order to optimize photon to electron conversion efficiency.

Acknowledgement

The authors would like to thank the State Key Program of Fundamental Research (G1998061310), the NNSFC-(20023005, 59872001) and Doctoral Program Foundation of High Education (99000132) for the financial support of this work.

References

1 (*a*) B. O'Regan and M. Grätzel, *Nature (London)*, 1991, **353**, 737–740; (*b*) M. K. Nazeeruddin, K. Kay, I. Rodicio, B. R. Humphry, E. Mueller, N. Vlachopolous and M. Grätzel, *J. Am. Chem. Soc.*, 1993, **115**, 6382.
2 G. J. Meyer and P. C. Searson, *Interface*, 1993, 23–27.
3 P. V. Kamat, I. Bedja, S. Hotchandani and L. K. Patterson, *J. Phys. Chem. B*, 1996, **100**, 4900–4908.
4 R. Hoyle, J. Sotomayer, G. Will and D. Fitzmaurice, *J. Phys. Chem. B*, 1997, **101**, 10791–10800.
5 C. Nasr, S. Hotchandani, W. Y. Kim, R. H. Schmehl and P. V. Kamat, *J. Phys. Chem.*, 1997, **101**, 7480.
6 G. Sauve, M. E. Cass, S. J. Doig, I. Lauermann, K. Pomykal and N. S. Lewis, *J. Phys. Chem. B*, 2000, **104**, 3488.
7 I. Bedja, P. V. Kamat, X. Hua, A. G. Lappin and S. Hotchandani, *Langmuir*, 1997, **13**, 2398.
8 (*a*) Z. S. Wang, C. H. Huang, Y. Y. Huang, Y. J. Hou, P. H. Xie, B. W. Zhang and H. M. Cheng, *Chem. Mater.*, 2001, **13**, 678; (*b*) Z. S. Wang, C. H. Huang, F. Y. Li, S. F. Weng, K. Ibrahim and F. Q. Liu, *J. Phys. Chem. B*, 2001, **105**, 4230–4234; (*c*) Z. S. Wang, C. H. Huang, F. Y. Li, S. F. Weng and S. M. Yang, *J. Photochem. Photobiol. A: Chem.*, 2001, **140**(3), 255–262; (*d*) Z. S. Wang, C. H. Huang, B. W. Zhang, Y. J. Hou, P. H. Xie, H. J. Qian and K. Ibrahim, *New J. Chem.*, 2000, **24**, 567.
9 R. Vogel, P. Hoyer and H. Weller, *J. Phys. Chem.*, 1994, **98**, 3183.
10 R. Suarez, P. K. Nair and P. V. Kamat, *Langmuir*, 1998, **14**, 3236.
11 B. O'Regan and D. T. Schwartz, *Chem. Mater.*, 1995, **7**, 1349–1354.
12 S. Ferrere, Arie. Zaban and B. A. Gregg, *J. Phys. Chem. B*, 1997, **100**, 4490–4493.
13 A. Kay and M. Grätzel, *J. Phys. Chem.*, 1993, **97**, 6272–6277.
14 K. Sayama, K. Hara, N. Mori, M. Satsuki, S. Suga, S. Tsukagoshi, Y. Abe, H. Sugihara and H. Arakawa, *Chem. Commun.*, 2000, 1173.
15 (*a*) Z. S Wang, F. Y. Li, C. H. Huang, L. Wang, M. Wei, L. P. Jin and N. Q. Li, *J. Phys. Chem. B*, 2000, **104**, 9676; (*b*) Z. S. Wang, F. Y. Li and C. H. Huang, *Chem. Commun.*, 2000, 2063.
16 F. G. Gao, A. J. Bard and L. D. Kispert, *J. Photochem. Photobiol. A: Chem.*, 1999, **130**, 49.
17 K. Hara, T. Horiguchi, T. Kinoshita, K. Sayama, H. Sugihara and H. Arakawa, *Sol. Energy Mater. Sol. Cells*, 2000, **64**, 115.
18 H. Gerischer, M. E. Michel-Beyerle, F. Rebentrost and H. Tributsch, *Electrochim. Acta*, 1968, **13**, 1509.
19 H. Tributsch and H. Gerischer, *Ber. Bunsen-Ges. Phys. Chem.*, 1969, **73**, 251.
20 H. Tsubomura, M. Matsumura, Y. T. Nomura and T. Amamiya, *Nature*, 1976, **261**, 402.
21 N. J. Cherepy, G. P. Smestad, M. Grätzel and J. Z. Zhang, *J. Phys. Chem.*, 1997, **101**, 9342.
22 C. Nasr, D. Liu, S. Hotchandani and P. V. Kamat, *J. Phys. Chem.*, 1996, **100**, 11054.
23 A. C. Khazraji, S. Hotchandani, S. Das and P. V. Kamat, *J. Phys. Chem.*, 1999, **103**, 4693.
24 K. Tennakone, A. R. Kumarasinghe, G. R. R. A. Kumara, K. G. U. Wijayantha and P. M. Sirimanne, *J. Photochem. Photobiol. A: Chem.*, 1997, **108**, 193.
25 K. Tennakone, G. R. R. A. Kumara, I. R. M. Kottegoda, V. P. S. Perera and P. S. R. S. Weerasundara, *J. Photochem. Photobiol. A: Chem.*, 1998, **117**, 137.
26 K. Sayama, M. Sugino, H. Sugihara, Y. Abe and H. Arakawa, *Chem. Lett.*, 1998, 753.
27 K. Hara, T. Horiguchi, T. Kinoshita, K. Sayama, H. Sugihara and H. Arakawa, *Chem. Lett.*, 2000, 316.
28 P. V. Kamat, *CHEMTECH*, 1995(June), 22.
29 A. Hagfeldt and M. Grätzel, *Chem. Rev.*, 1995, **95**, 49.
30 H. Weller, *Angew. Chem., Int. Ed. Engl.*, 1993, **32**, 41–53.
31 S. Gallardo, M. Gutierrez, A. Henglein and E. Janata, *Ber. Bunsen-Ges. Phys. Chem.*, 1989, **93**, 1080–1090.
32 S. M. Yang, Z. S. Wang and C. H. Huang, *Synth. Met.*, 2001, **123**, 267–272.
33 R. Vogel, K. Pohl and H. Weller, *Chem. Phys. Lett.*, 1990, **174**, 241.
34 A. K. Ghosh, D. L. Morel, T. Feng, R. F. Shaw and C. A. Rowe, *J. Appl. Phys.*, 1974, **45**, 230.

35 M. L. Rosenbluth and N. S. Lewis, *J. Phys. Chem.*, 1989, **93**, 3735.
36 M. X. Tan, P. E. Laibinis, S. T. Nguyen, J. M. Kesselman, C. E. Stanton and N. S. Lewis, *Prog. Inorg. Chem.*, 1994, **41**, 21.
37 B. O'Regan, J. Moser, M. Anderson and M. Grätzel, *J. Phys. Chem.*, 1990, **94**, 8720.
38 S. Sodergren, A. Hagfeldt, J. Olsson and S.-E. Lindquist, *J. Phys. Chem.*, 1994, **98**, 5552.
39 L. Spanhel, M. Hasse, H. Weller and A. Henglein, *J. Am. Chem. Soc.*, 1987, **109**, 5649.